

Surface Science

Magnetic Structure

Cu metallic quantum well states on Cu/Ni/Cu(100) and Cu/Fe/Cu(100)

Danese, A., R.A. Bartynski, D.A. Arena, M. Hochstrasser, J. Tobin

Determination of formal oxidation state of Co in MBE-grown co-doped TiO₂(001) anatase epitaxial films by x-ray absorption spectroscopy

Chambers, S.A., T. Droubay, S. Thevuthasan, N.H. Hamdan

Investigation of surface and bulk half-metallic character of Fe₃O₄ by spin resolved photoemission

Morton, S.A., G.D. Waddill, S. Kim, I.K. Schuller, S.A. Chambers, J.G. Tobin

Magnetic circular dichroism in the x-ray absorption spectra of the CMR compound, Yb₁₄MnSb₁₁

Holm, A.P., S.M. Kauzlarich, S.A. Morton, G.D. Waddill, W.E. Pickett, J.G. Tobin

Magnetic properties of Fe₃O₄ films grown by epitaxial electrodeposition on the low index planes of gold

Switzer, J.A., T.A. Sorenson, S.A. Morton, G.D. Waddill

Photoemission electron microscopy and x-ray magnetic circular dichroism of Fe_xNi_(1-x) thin films on Cu(111)

Sato, Y., T.F. Johnson, S. Chiang, X.D. Zhu, D.P. Land, J.A. Giacomo, F. Nolting, A. Scholl

Spin-resolved electronic structure studies of ultrathin films of Fe on singular and vicinal GaAs

Spangenberg, M., E.A. Seddon, E.M.M. McCash, T. Shen, S.A. Morton, D. Waddill, J. Tobin

Variable moments and changing magnetic behavior of thin-film FeNi alloys

Hochstrasser, M., J.G. Tobin, N.A.R. Gilman, R.F. Willis, S.A. Morton, G.D. Waddill

X-ray magnetic linear dichroism of Fe-Ni alloys on Cu(111)

Johnson, T.F., Y. Sato, S. Chiang, M. Hochstrasser, J.G. Tobin, J.A. Giacomo, J.D. Shine, X.D. Zhu, D.P. Land, D.A. Arena, S.A. Morton, G.D. Waddill

Cu Metallic Quantum Well States on Cu/Ni/Cu(100) and Cu/Fe/Cu(100)

A. Danese,¹ R.A. Bartynski,¹ D.A. Arena,² M. Hochstrasser,² and J. Tobin²

¹Department of Physics and Laboratory for Surface Modification
Rutgers University, 136 Frelinghuysen Rd., Piscataway, NJ 08855

²Lawrence Livermore National Laboratory

Ultrathin metal films grown epitaxially on metal substrates often exhibit so called metallic quantum well (MQW) states.[1-8] These are electronic states that are confined to the overlayer by reflectivity from projected band gaps in the substrate metal. Even in the absence of such band gaps, significant interface reflectivity can from intense quantum well resonances. Owing to band structure effects, a given MQW state will move to higher energy as the thickness of the overlayer increases. Furthermore, the periodicity with which these states cross the Fermi level is expected to be a function of the overlayer band structure and insensitive to the substrate.

Much of the work on MQW states has concentrated on the behavior of Cu on various transition metal substrates such as Ni and Co, owing to their importance in magnetic multilayers. In the unoccupied electronic states above the Fermi level, the Cu/Ni(100) system is unusual in that the Cu-induced levels disperse downward with increasing film thickness, rather than upward.[9, 10] It was thought that this might be due to strain in the Cu film. To test these ideas, we used photoemission and inverse photoemission to study the occupied and unoccupied overlayer electronic states of the Cu/Ni/Cu(100) system as a function of Cu and Ni thickness.

In Fig. 1 we show inverse photoemission spectra from increasingly thick Cu overlayers on a 35 ML and on a 5 ML film of Ni grown on Cu(100). One can see that the results are qualitatively similar to each other, and to the Cu/Ni(100) results, in that the Cu-induced states disperse downward as a function of increasing Cu film thickness. There are quantitative differences, however. The states of the Cu films grown on the thinner Ni layer are at higher energy than those on the thicker Ni film. Although it appears that the downward dispersion does not appear to arise from a strain effect, these quantitative differences may. To test this, we measured normal emission photoemission from wedges of Cu grown on two different thickness Ni films on the same Cu(100) substrate. A diagram of the sample geometry is shown in Fig. 2. Two identical Cu wedges were grown on Ni films of 7 ML and 35 ML thicknesses.

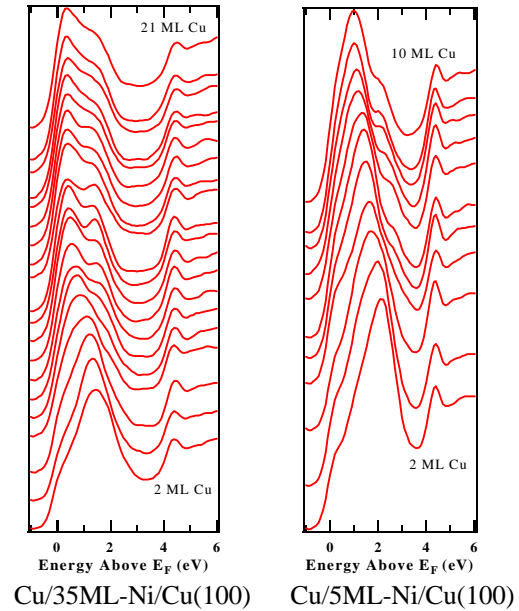


Fig. 1: Downward dispersion of unoccupied Cu states in the Cu/Ni/Cu(100) system.

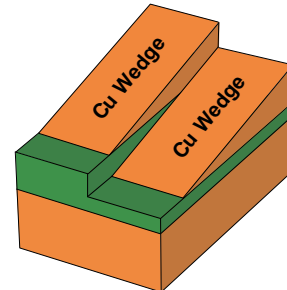


FIG.2: Sample geometry for photoemission studies.

Using the UltraESCA end station of Beamline 7.0.1, we have obtained photoemission data from the Cu/fccNi/Cu(100) system. The sample was prepared by depositing the Ni onto an atomically

clean, well-ordered Cu(100) surface. This was followed by deposition of a wedge-shaped Cu film whose thickness ranged from 0 to 40+ ML. Figure 3 show a series of normal emission photoemission data displayed as a 2-dimensional plot of Cu film thickness vs. binding energy. Light colors indicate high intensity and the dark colors low. These peaks are associated with metallic quantum well states in the Cu films. In contrast to the inverse photoemission data, the intensity maxima that move towards the Fermi level as the film thickness increases. Although the MQW states are less pronounced on the thicker Ni film, the period with which these Cu MQW states cross E_F appears are identical. As a change in the Cu lattice constant would change the electronic structure and thus change the periodicity of the Fermi level crossings, these results suggest that there is minimal change in strain in these Cu films. Strain in the Ni, however, may cause this effect. Quantitative structural studies and first principles electronic structure calculations are currently underway to investigate the low energy structures of these systems.

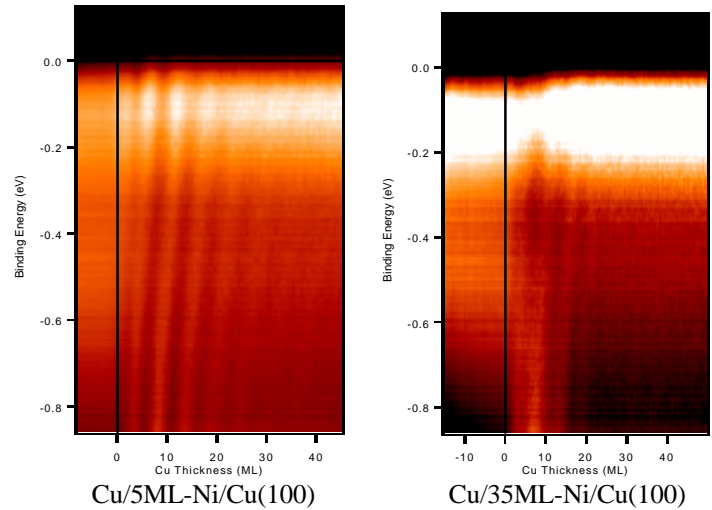


Fig. 3.: Normal emission from the Cu/Ni/Cu(100) systems as a function of Cu film thickness.

Another important observation is the sharp contrast between the upward dispersion of Cu MQW states below the Fermi level and the downward dispersion of Cu state above E_F . Most likely this difference arises because the Ni d -bands terminate about $E_F + 0.1$ eV. The downward dispersion if the Cu states on Ni is most likely associated with the interaction of the Cu and Ni sp -band.

Finally, we have also grown Cu/fccFe/Cu(100) quantum well structures and they exhibit a strong upward dispersion and cross E_F with a periodicity that is, within experimental uncertainty, the same as that of the Cu/Ni system.

REFERENCES

- [1] J.E. Ortega and F.J. Himpsel, Phys. Rev. Lett. **69**, 844 (1992).
- [2] P. Segovia, E.G. Michel and J.E. Ortega, Phys. Rev. Lett. **77**, 2734 (1996).
- [3] F.G. Curti, A. Danese and R.A. Bartynski, Phys. Rev. Lett. **80**, 2213 (1998).
- [4] R.K. Kawakami et al., Phys. Rev. Lett. **80**, 1754 (1998).
- [5] R.K. Kawakami et al., Nature. **398**, 132 (1999)
- [6] R.K. Kawakami et al., Phys. Rev. Lett. **82**, 4098 (1999).
- [7] A. Danese and R.A. Bartynski, Phys. Rev. B. (in press).
- [8] A. Danese, D.A. Arena and R.A. Bartynski, Prog. Surf. Sci. **67**, 249 (2001).
- [9] O. Rader and F.J. Himpsel, Appl. Phys. Lett. **67**, 1151 (1995).
- [10] C. Hwang and F.J. Himpsel, Phys. Rev. B **52**, 15368 (1995).

This work is supported by NSF Grant DMR-98-01681 and Petroleum Research Fund Grant # 33750-AC5,6.

Principle Investigator: Robert A. Bartynski, Department of Physics and Laboratory for Surface Modification, Rutgers University. Email: bart@physics.rutgers.edu. Telephone: 732-445-4839

Determination of Formal Oxidation State of Co in MBE-Grown Co-doped TiO₂(001) Anatase Epitaxial Films by X-ray Absorption Spectroscopy

S.A. Chambers¹, T. Droubay¹, S. Thevuthasan¹, N.H. Hamdan²

¹Fundamental Science Division, Pacific Northwest National Laboratory
Richland, WA 99352, U.S.A.

²Lawrence Berkeley National Laboratory, Berkeley, CA 94720, U.S.A.

INTRODUCTION

Diluted magnetic semiconductors (DMS) consist of nonmagnetic semiconducting materials doped with a few atomic percent of impurity magnetic cations. Magnetic coupling occurs by virtue of exchange interactions between the magnetic spins and free carriers in the semiconductor. The interaction can occur via *p-d* or *d-d* exchange, and can lead to antiferromagnetic or ferromagnetic coupling, depending on the concentration and the local structural environment of the magnetic impurity. DMS materials grown as thin epitaxial films can be used as spin injectors for semiconductor heterostructures, provided they are ferromagnetic.

Virtually all conventional DMS materials exhibit Curie temperatures of ~100K or less and must be *p*-type, which means that the exchange interaction leading to ferromagnetic behavior is hole mediated. Most of the effort expended to date on understanding the crystal growth and properties of thin-film DMS materials has focused on Mn-doped II-VI, III-V, and Group IV semiconductors.¹⁻⁴ Relatively little effort has gone into the investigation of “nontraditional” semiconductors, such as semiconducting oxides, to see if they are more robust magnetically. However, one such oxide - Co-doped TiO₂ anatase (Co_xTi_{1-x}O₂) - has recently been discovered to be the most magnetically robust DMS with regard to magnetic moment at saturation, coercivity, remanence, and Curie temperature.⁵ Indeed, it is one of the very few DMS materials demonstrated to exhibit ferromagnetic behavior above 300K. In addition, it has been shown that the material can be grown epitaxially by both pulsed laser deposition (PLD)⁶ and oxygen plasma assisted molecular beam epitaxy (OPA-MBE)⁵ on SrTiO₃(001) and LaAlO₃(001). However, the resulting magnetic properties differed considerably for the two growth methods, with significantly better properties exhibited by OPA-MBE grown material.

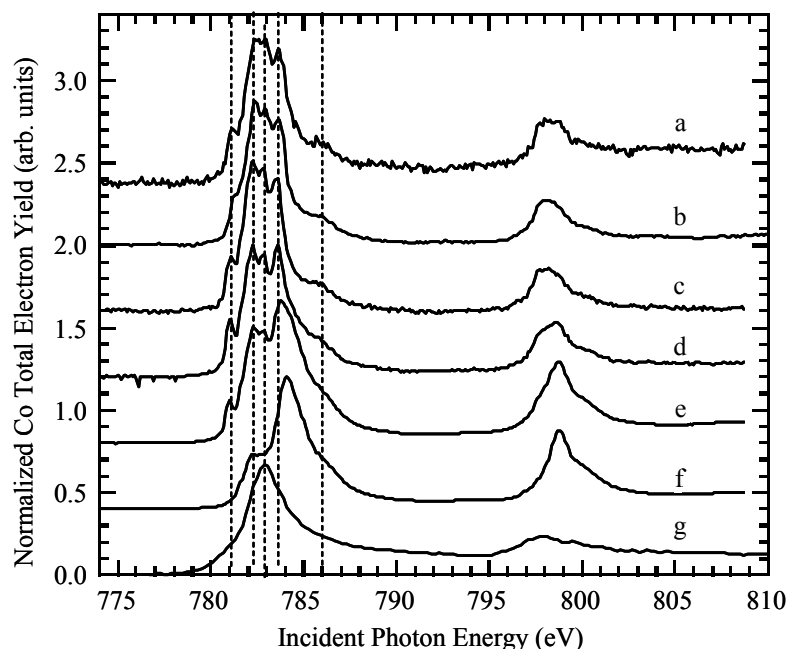
In order to understand the mechanism of magnetism in this fascinating material, it is essential to know the charge state of the magnetic cation (Co), and the doping type. We have utilized Co L-edge x-ray absorption spectroscopy (XAS) at beamline 9.3.2 to determine the Co charge state.

EXPERIMENT

Epitaxial Co_xTi_{1-x}O_{2-x} films of high structural quality were grown by OPA-MBE on LaAlO₃(001)⁷ using a system at PNNL described in detail elsewhere.⁸ The resulting samples were then transferred through air to beamline 9.3.2 and XAS measurements were made in total electron yield mode at the Co L-edge, Ti L-edge, and O K-edge. X-ray absorption near-edge spectra (XANES) were also recorded for several Co standards for comparison purposes. No surface cleaning was done, as the distribution of Co has been shown to be strongly modified by post-growth annealing at the temperatures required to rid the surface of carbon, or remove sputter damage.

RESULTS

We show in Fig. 1 Co L-edge XAS data for three films with different Co mole fractions (x) (Fig. 1a-c), and for standards containing Co in different oxidation states and local structural environments (Fig. 1d-g). The CoTiO_3 standard was a powder, CoO was a (001)-oriented bulk single crystal, $\gamma\text{-Co}_2\text{O}_3$ was a 100 nm thick (001)-oriented epitaxial film grown on $\text{MgO}(001)$ at PNNL, and the Co metal standard was a polycrystalline film evaporated *in situ* in the XAS chamber. Comparison of all film spectra with those for the standards reveals a good fit with both CoTiO_3 and CoO , which both contain Co^{+2} , but a very poor fit for both $\gamma\text{-Co}_2\text{O}_3$, which contains Co^{+3} , and for Co metal. The fit to CoTiO_3 is better than that to CoO . However, there is some similarity between the reference spectra for CoO and $\gamma\text{-Co}_2\text{O}_3$, particularly in the vicinity of the feature at 784 eV. This result indicates that there may be some Co^{+3} in the CoO single crystal. The very high degree of similarity between the spectra for the Co-doped anatase films and the CoTiO_3 standard establishes that Co in the former is in the +2 formal oxidation state. Interestingly, using the Co evaporation rate and oxygen plasma beam intensity we have used for the growth of $\text{Co}_x\text{Ti}_{1-x}\text{O}_{2-x}$ result in the epitaxial growth of metastable $\gamma\text{-Co}_2\text{O}_3$ on $\text{MgO}(001)$. Therefore, the anatase lattice stabilizes the formation of Co(II) , even though the conditions would result in Co(III) formation if pure Co oxide were allowed to grow under comparable



conditions.

Fig. 1 Co L-edge XAS for 20 nm thick films of epitaxial $\text{Co}_x\text{Ti}_{1-x}\text{O}_{2-x}$ on $\text{LaAlO}_3(001)$: (a) $x = 0.01$, (b) $x = 0.06$, (c) $x = 0.08$. Also shown are spectra for reference compounds containing Co in different formal oxidation states: (d) CoTiO_3 , (e) CoO , (f) $\gamma\text{-Co}_2\text{O}_3$, and (g) Co metal.

SIGNIFICANCE

Ion channeling measurements conducted at PNNL reveals that Co substitutes for Ti in the anatase lattice. Furthermore, Hall effect measurements carried out at PNNL show that these films are *n*-type semiconductors as grown, despite the fact that no intentional *n*-type doping was carried out. The origin of the *n*-type doping may have to do with the presence of H in the film,

which has been detected by ^{19}F nuclear reaction analysis at PNNL at a concentration that is of the same order of magnitude as that of the free carriers – 10^{19} to 10^{20} cm^{-3} . H may be the direct dopant, as occurs in $n\text{-ZnO}$.⁹ Alternatively, H_2 , which is present in the growth chamber at a very low partial pressure, may partially reduce lattice oxygen during growth to produce OH and a free donor electron according to the reaction $\text{O}^{2-}_{(\text{lattice})} + (1/2)\text{H}_2 \rightarrow \text{OH}^{-}_{(\text{lattice})} + \text{e}^{-}$. This phenomenon is currently under more detailed investigation.

It thus appears that Co-doped anatase TiO_2 is ferromagnetic by virtue of *electron* mediated exchange interaction between Co^{+2} cations that substitute for Ti^{+4} in the lattice. In order to maintain charge neutrality, each substitutional Co^{+2} must be accompanied by an O^{2-} vacancy. However, such vacancies are uncharged and therefore do not contribute any donor electrons. In fact, n -type semiconducting behavior and Co substitution are independent phenomena; some highly resistive films are nonmagnetic despite having several at. % Co. Indeed, the magnetization depends as much on the free carrier concentration as on the presence of substitutional Co, as expected for a DMS.

Significantly, virtually all other known DMS materials are ferromagnetic by virtue of *hole* mediated exchange interaction, which has been thought to be the stronger interaction.¹⁰ Therefore, Co-doped TiO_2 anatase is a highly unusual and potentially very important DMS in that it exhibits strong electron mediated exchange interaction at temperatures of at least 500K. No other known DMS exhibits these properties.

REFERENCES

1. R. Fiederling, M. Keim, G. Reuscher, W. Ossau, G. Schmidt, A. Waag, L.W. Molenkamp, *Nature* **402**, 787 (1999).
2. B.T. Jonker, Y.D. Park, B.R. Bennett, H.D. Cheong, G. Kioseoglou, A. Petrou, *Phys. Rev. B* **62**, 8180 (2000).
3. R.K. Kawakami, Y. Kato, M. Hanson, I. Malajovich, J.M. Stephens, E. Johnston-Halperin, G. Salis, A.C. Gossard, D.D. Awschalom, *Science* **294**, 131 (2001).
4. Y.D. Park, A.T. Hanbicki, S.C. Irwin, C.S. Hellberg, J.M. Sullivan, J.E. Mattson, T.F. Ambrose, A. Wilson, G. Spanos, B.T. Jonker, *Science* **295**, 651 (2002).
5. S.A. Chambers, S. Thevuthasan, R.F.C. Farrow, R.F. Marks, J.-U. Thiele, L. Folks, M.G. Samant, A.J. Kellock, N. Ruzyski, D.L. Ederer, U. Diebold, *Appl. Phys. Lett.* **79**, 3467 (2001), and, S.A. Chambers, *Mat. Today*, to appear, April issue (2002).
6. Y. Matsumoto, M. Murakami, T. Shono, T. Hasegawa, T. Fukumura, M. Kawasaki, P. Ahmet, T. Chikyow, S.-Y. Koshihara, H. Koinuma, *Science* **291**, 854 (2001).
7. S.A. Chambers, C. Wang, S. Thevuthasan, T. Droubay, D.E. McCready, A.S. Lea, V. Shutthanandan, C.F. Windisch, Jr., submitted to *Thin Solid Films* (2002).
8. S.A. Chambers, *Surf. Sci. Rep.* **39**, 105 (2000).
9. D.M. Hofman, A. Hofstaetter, F. Lieter, H. Zhou, F. Henecker, B.K. Meyer, S.B. Orlinskii, J. Schmidt, and P.G. Baranov, *Phys. Rev. Lett.* **88**, 045504-1 (2002).
10. T. Dietl, H. Ohno, F. Matsukura, J. Cibert and D. Ferrand, *Science* **287**, 1019 (2000).

The work was funded by a Laboratory Directed Research and Development grant associated with the PNNL Nanoscience and Technology Initiative, and by DOE BES Materials Science.

Principal Investigator – S.A. Chambers. Phone – (509) 376-1766. E-mail – sa.chambers@pnl.gov

Investigation of Surface and Bulk Half-metallic Character of Fe_3O_4 by Spin Resolved Photoemission

S. A. Morton (a), G. D. Waddill (a), S. Kim (b), Ivan K. Schuller (b), S. A. Chambers (c) and J. G. Tobin (d)

(a) Department of Physics, U. of Missouri-Rolla, Rolla, MO 65409, USA

(b) Department of Physics, U. of California San Diego, La Jolla, CA 92093, USA

(c) Pacific Northwest National Laboratory, Richland, WA 99392, USA

(d) Lawrence Livermore National Laboratory, Livermore, CA 94550 USA

The existence of a new class of magnetic materials displaying metallic character for one electron spin population and insulating character for the other was first postulated by DeGroot *et al* [1] in 1983 based on theoretical band structure calculations of the ferromagnetic Heusler alloy NiMnSb. Since then such half metallic materials, which by definition possess 100% electron polarization at the Fermi energy have attracted considerable theoretical, experimental, and technological interest as potential pure spin sources for use in spintronic devices [2], data storage applications, and magnetic sensors. In addition to Heusler alloys half metallic character has also been predicted to occur in a wide range of manganites [3], metallic oxides [4], and CMR systems [5]. However, such predictions have proven to be extremely difficult to confirm experimentally [6]. A major factor in this failure has proven to be significant experimental challenges in obtaining a clean stoichiometric surface with a magnetization that is truly representative of the bulk material and thus suitable for further study by magneto-optical or spectroscopic techniques.

In recent experiments at the ALS we have used spin resolved photoemission to study the role that surface reconstruction plays in the observed polarization of the half metallic candidate material magnetite, Fe_3O_4 . Magnetite has a structure that is relatively simple in comparison to most other candidate half metals and it can be grown epitaxially using conventional deposition techniques [7], making it one of the strongest candidates for spintronic applications. However previous spin resolved measurements have shown that the polarization at the Fermi edge is only ~40% [8] rather than the anticipated 100%.

By conducting spin resolved depth profile measurements and comparing the results to theoretical band structure calculations we have demonstrated that Fe_3O_4 exhibits a semiconducting non-magnetic surface re-construction which significantly reduces the observed polarization but that, in contrast, the underlying bulk material is in fact very strongly polarized. Indeed, once the effects of this surface reconstruction are taken into account by theoretical models of the polarization an excellent match is obtained between the experimental spin resolved spectra and simulated spectra generated from theoretical spin polarized band structure calculations [9] (fig. 1). Hence our results strongly support the notion that Fe_3O_4 is indeed a half-metallic material suitable for use in a new generation of spintronic devices.

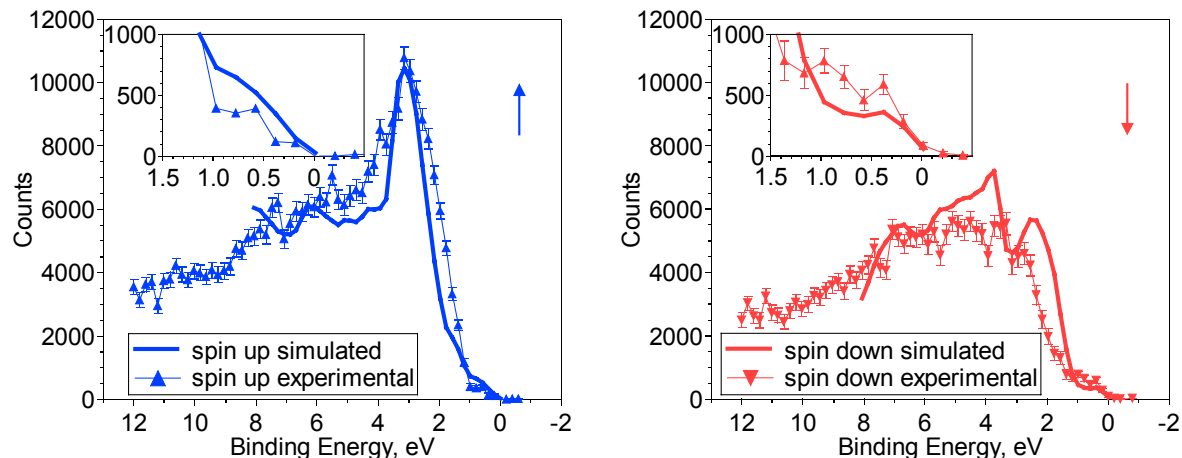


Figure 1

Comparison of experimental spin resolved Fe_3O_4 valence bands with equivalent simulated spectra derived from theoretical calculations that have been corrected to account for the presences of a nonmagnetic surface reconstruction

References

1. R. A. de Groot *et al.*, *Phys. Rev. Lett.* **50**, 2024 (1983).
2. S. A. Wolf, D. Treger, *IEEE Trans. Mag.* **36** 2748 (2000).
3. S. Jin *et al.*, *Science* **264**, 413 (1994).
4. Z Zhang, S. Satpathy, *Phys. Rev. B* **44**, 13319 (1991).
5. W. E. Pickett, D. J. Singh, *Phys. Rev. B* **53**, 1146 (1996).
6. K. P. Kamper *et al.*, *Phys. Rev. Lett.* **59** 2788 (1987).
7. S. A. Chambers, S. A. Joyce, *Surf. Sci.* **420**, 111 (1999).
8. S. F. Alvarado *et al.*, *Phys. Rev. Lett.* **34**, 319 (1975).
9. S.A. Morton *et al.*, *Submitted to Surface Science Letters*

This work was supported by the Director, Office of Energy Research, Office of Basic Energy Sciences, Materials Science Division, of the U.S. Department of Energy under Contract No. # R5-32633.A02. This work was performed under the auspices of the U.S Department of Energy by Lawrence Livermore National Laboratory under contract no. W-7405-Eng-48.

Principal Investigator: Ivan K. Schuller, Department of Physics, University of California San Diego, La Jolla, CA 92093. Phone: (858) 534-2540 fax: (858) 534-0173 Email: ischuller@ucsd.edu

Magnetic Circular Dichroism in the X-ray Absorption Spectra of the CMR Compound, $\text{Yb}_{14}\text{MnSb}_{11}$

A. P. Holm¹; S. M. Kauzlarich¹; S. A. Morton²; G. D. Waddill³;
W. E. Pickett⁴; J. G. Tobin²

¹Department of Chemistry, University of California, Davis, CA 95616.

²Lawrence Livermore National Laboratory, Livermore, CA 94550.

³Department of Physics, University of Missouri-Rolla, Rolla, MO 65401-0249.

⁴Department of Physics, University of California, Davis, CA 95616.

This work is part of ongoing investigations into the magnetic and electronic properties of the rare-earth transition metal Zintl phases $\text{A}_{14}\text{MnPn}_{11}$ ($\text{A} = \text{Eu}, \text{Yb}$; $\text{Pn} = \text{Sb}, \text{Bi}$) at the Advanced Light Source. We have recently obtained exciting new results from X-ray magnetic circular dichroism (XMCD) investigations of the $\text{Yb}_{14}\text{MnSb}_{11}$ system. Specifically, we have used XMCD as an element specific probe into the nature of the magnetic moment in this system with the intention of exploring the proposed half-metallic nature of this compound and its related substitutional analogues. Our XMCD measurements indicate that $\text{Yb}_{14}\text{MnSb}_{11}$ is a half-metallic ferromagnet, and we have submitted our results for publication to Physical Review Letters.

The term half-metallic ferromagnet arises from theoretical predictions made by R.A. de Groot et al based on band structure calculations of the ferromagnetic Heusler alloy NiMnSb .¹ These calculations proposed a new phase of matter that displays separate electronic properties for majority-spin and minority-spin electrons. Specifically, one electron spin population is metallic and the other is insulating. Such a material, (possessing 100% spin polarization of the conduction electron) would hold significant technological potential as a single-spin electron source for spintronic devices, data storage applications, and high efficiency magnetic sensors.²

The materials we are studying are new compounds that belong to a class of materials called transition-metal Zintl phases. These compounds are isostructural to $\text{Ca}_{14}\text{AlSb}_{11}$ and crystallize in the tetragonal space group $I4_1/a$ ($Z = 8$). The $\text{Yb}_{14}\text{MnSb}_{11}$, $\text{Yb}_{14}\text{MnBi}_{11}$ and $\text{Eu}_{14}\text{MnSb}_{11}$ analogues are each reported to order ferromagnetically at 56 K, 58 K and 28 K, and 92 K, respectively.³⁻⁶ $\text{Eu}_{14}\text{MnBi}_{11}$ is an antiferromagnet with a Néel transition at $T_N = 32$ K.⁶ Each of these materials exhibits a large resistance drop associated with their unique magnetic ordering temperature. This behavior is attributed to colossal magnetoresistance effects, and could help support the proposal made by Pickett and Singh of a correlation between half-metallicity and colossal magnetoresistance.⁷ These systems are ideal for investigations into the links between magneto-resistance, magnetic moment and half-metallic behavior.

The ability to perform X-ray magnetic circular dichroism experiments on the EPU has allowed us to probe the dichroic characteristics of Mn and Sb in the $\text{Yb}_{14}\text{MnSb}_{11}$

system during experiments recently performed on beamline 4.0 of the ALS. Figure 1 shows the results from XMCD experiments on the Mn L_{23} , Sb M_{45} , and Yb N_{45} edges of $\text{Yb}_{14}\text{MnSb}_{11}$. A dramatic dichroism effect is shown in the Mn L_{23} region which is confined to one sub-component of the Mn edge and closely matches theoretical models for Mn^{2+} , d^5 dichroism (Figure 1d). The difference in intensity upon change of helicity is greater than 30%, and is strong evidence of a significant moment being present on the Mn. In contrast, no dichroism was observed in the Yb edges, but a small antialigned moment is present in the Sb M_{45} edges as shown on the left side of Figure 1. This result is surprising because initial models predicted that dichroism would be restricted to the Mn L_{23} region (with no dichroism in the Sb M_{45} region) and that it would be Mn^{3+} , d^4 like in character. However, an ongoing collaboration with theoretical groups in the physics departments of the University of California, Davis and the University of Illinois, Urbana to model the Ca and Ba analogues of this structure type has now produced calculated results consistent with our experimental observations of how the Sb behaves in this system. They argue that the Mn should be in a $2+$, d^5 configuration, and the Sb_4 cage surrounding the Mn should have a hole antialigned to the Mn moment giving a total moment of $\sim 4 \mu_B/\text{formula unit}$. Our experimental results are consistent with these new theoretical results, and in addition, these comparisons of data with theoretical calculations and SQUID magnetometry measurements confirm that $\text{Yb}_{14}\text{MnSb}_{11}$ is indeed a half-metallic ferromagnet.⁸⁻¹⁰

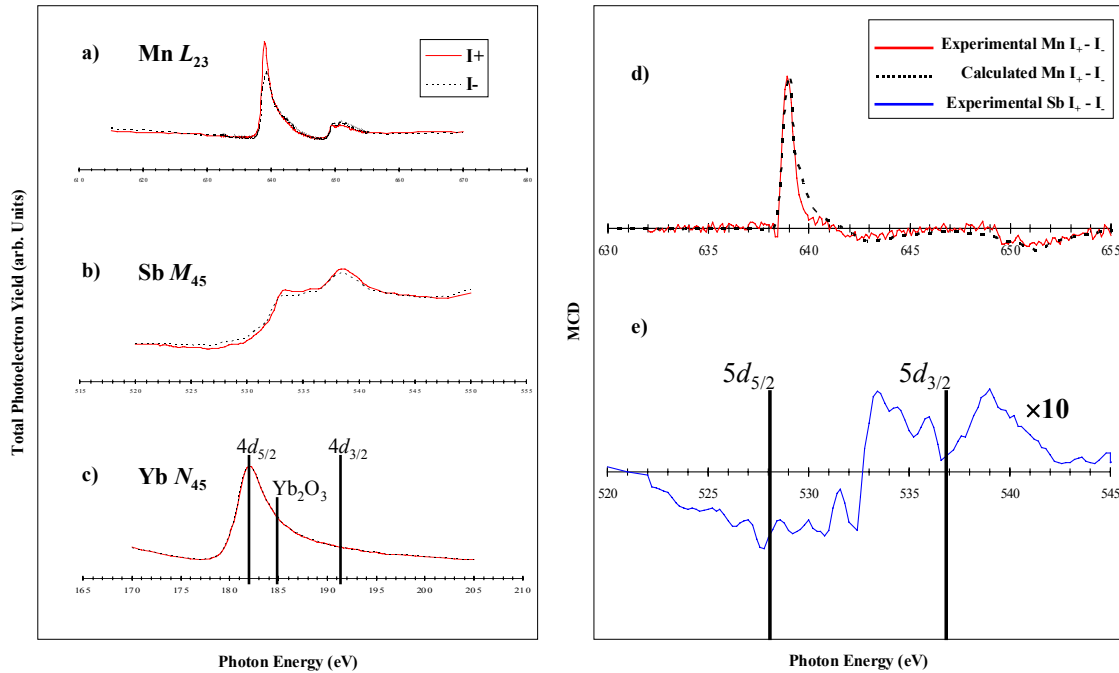


Fig. 1. The raw absorption spectra at plus and minus light polarization for a) Mn L_{23} , b) Sb M_{45} , and c) Yb N_{45} are shown on the left. The XMCD spectra for d) the experimental Mn L_{23} denoted by a solid red line and the calculated Mn^{2+} , d^5 L_{23} denoted by a dashed black line, and e) the experimental Sb M_{45} denoted by a solid blue line.¹⁰

References:

1. de Groot, R. A.; Mueller, F. M.; van Engen, P. G.; Buschow, K. H. J. *Physical Review Letters* **1983**, *50*, 2024 -2027.
2. Prinz, G. A. *Science* **1998**, *282*, 1660 - 1663.
3. Chan, J. Y.; Kauzlarich, S. M.; Klavins, P.; Shelton, R. N.; Webb, D. J. *Chemistry of Materials* **1997**, *9*, 3132-3135.
4. Chan, J. Y.; Olmstead, M. M.; Kauzlarich, S. M.; Webb, D. J. *Chemistry of Materials* **1997**, *10*, 3583 - 3588.
5. Chan, J. Y.; Wang, M. E.; Rehr, A.; Kauzlarich, S. M.; Webb, D. J. *Chemistry of Materials*. **1997**, *9*, 2131 - 2138.
6. Chan, J. Y.; Kauzlarich, S. M.; Klavins, P.; Shelton, R. N.; Webb, D. J. *Physical Review B* **1998**, *57*, 8103 - 8106.
7. Pickett, W. E.; Singh, D. J. *Physical Review B* **1996**, *53*, 1146 - 1160.
8. Sánchez-Portal, D.; Martin, R. M.; Kauzlarich, S. M.; Pickett, W. E. *Physical Review B* **2001**, *Submitted September 31*.
9. van der Laan, G.; Thole, B. T. *Physical Review B* **1991**, *43*, 13401-13411.
10. Holm, A. P.; Kauzlarich, S. M.; Morton, S. A.; Waddill, G. D.; Pickett, W. E.; Tobin, J. G. *Physical Review Letters* **2001**, *Submitted November 26*.

This work was supported by the Director, Office of Energy Research, Office of Basic Energy Sciences, Materials Science Division, of the U.S. Department of Energy under Contract No. # R5-32633.A02. This work was performed under the auspices of the U.S. Department of Energy by Lawrence Livermore National Laboratory under contract no. W-7405-Eng-48.

Principal Investigator: Susan M. Kauzlarich, Department of Chemistry, University of California Davis, California 95616. Phone: (530)752-4756 fax: (530)752-8995 Email: smkauzlarich@ucdavis.edu

Magnetic Properties of Fe₃O₄ Films Grown by Epitaxial Electrodeposition on the Low Index Planes of Gold

J.A. Switzer¹, T.A. Sorenson¹, S.A. Morton², and G.D. Waddill²

¹Department of Chemistry and Graduate Center for Materials Research

²Department of Physics and Graduate Center for Materials Research
University of Missouri-Rolla, Rolla, Missouri 65409-1170, USA

Spin-dependent charge transport is currently receiving a lot of attention due to potential applications in giant magnetoresistive (GMR) devices such as magnetic field sensors, magnetoresistive random access memories (MRAM), read heads, and galvanic isolators.^{1,2} These devices require a source of spin-polarized electrons. Magnetite, Fe₃O₄, is a promising source of spin-polarized carriers, because density-functional theory spin-resolved density of states calculations have suggested that electrons at the Fermi level are ~100% spin polarized.^{3,4} Magnetite is a mixed-valence 3d transition metal oxide that has an inverse spinel structure (space group *Fd3m*) with a lattice constant of 0.8397 nm. The tetrahedral sites of the spinel structure are entirely occupied by Fe³⁺, whereas the octahedral sites are occupied half by Fe²⁺ and half by Fe³⁺. Fe₃O₄ undergoes a metal-to-insulator Verwey transition at 120 K and the Curie temperature of magnetite is 860 K. Recently, GMR effects greater than 500% have been reported at room temperature for Fe₃O₄ nanocontacts.⁵

We have electrodeposited galvanostatically epitaxial Fe₃O₄ films on Au(111), a system with a 3% lattice mismatch.⁶ These films are ~0.5 μm thick and have a (111) orientation. X-ray diffraction and SEM results establish that the magnetite films consist of twinned domains rotated by 180° with respect to each other. For the spin-polarized photoemission measurements a magnetic field from an *in situ* electromagnet is applied to the sample either in the plane of the sample or perpendicular to that plane. The field is then removed and the photoemission measurements are performed in remanence. The spin-resolved measurements were done at Beamline 7.0.1 with the spin-resolved endstation.⁷ The energy of the excitation beam was ~160 eV. Emitted photoelectrons were collected and filtered by a PHI 10-360 SCA hemispherical electron energy analyzer and then passed into a micro-Mott detector to resolve the electron spins. The total energy resolution for the spin resolved measurements was ~0.5 eV. Finally we have measured Fe L edge and O K edge XAS as well as Fe MXCD for these samples at Beamline 4.0. For the MXCD measurements, the sample was magnetized *in situ* and the measurements were made in remanence. All measurements were made at room temperature. Prior to the photoemission, XAS, and MXCD measurements the samples are briefly sputtered and then annealed in an oxygen environment. This produces LEED patterns consistent with the presence of rotationally twinned Fe₃O₄(111), but the films are rather poorly ordered. Photoemission always observes a trace amount of surface carbon.

The Fe L edge and O K edge XAS are shown in Figs. 1 and 2 respectively. In Fig. 3 we show the Fe L edge MXCD. These results are virtually indistinguishable from results reported by Kim *et al.* for a bulk magnetite sample.⁸ Figs. 4 and 5 show the spin-resolved photoemission results for these samples. The polarization at the Fermi level is approximately –40% with a change in the sign of the polarization observed at ~1 eV binding energy. The reasons for the observed deviation from the predicted value of –100% is not known. There are two recent reports for *in situ* prepared Fe₃O₄ films that report either –50%⁹ or –80%¹⁰ spin-polarization. The first result

is attributed to correlation effects that set an upper limit on the spin-polarization of -67% ¹¹ while the latter is regarded as evidence for half-metallic behavior. The discrepancy between these various results requires further investigation.

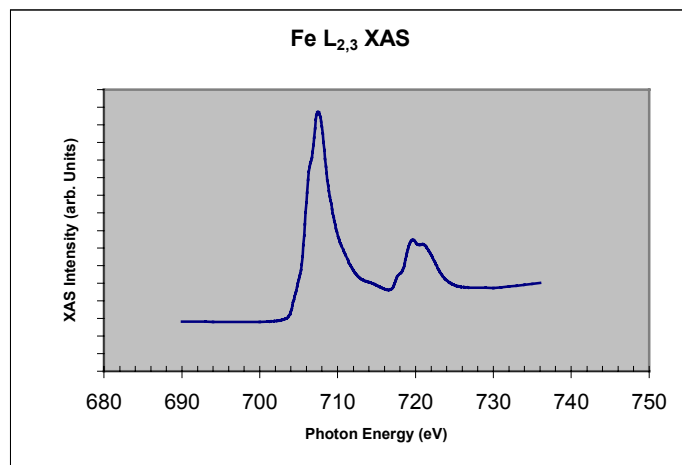


Figure 1. Fe L edge x-ray absorption for thick magnetite film on Au(111).

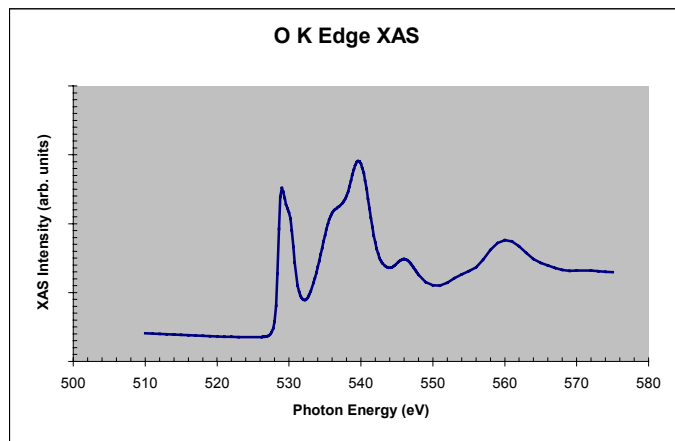


Figure 2. O K edge x-ray absorption for thick magnetite film on Au(111).

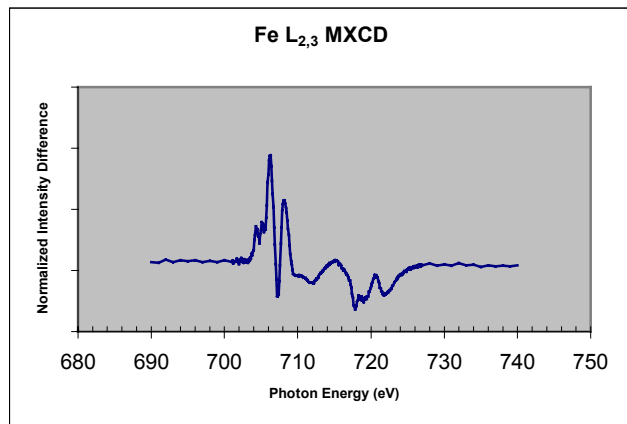


Figure 3. Fe L edge magnetic x-ray circular dichroism for thick magnetite film on Au(111).

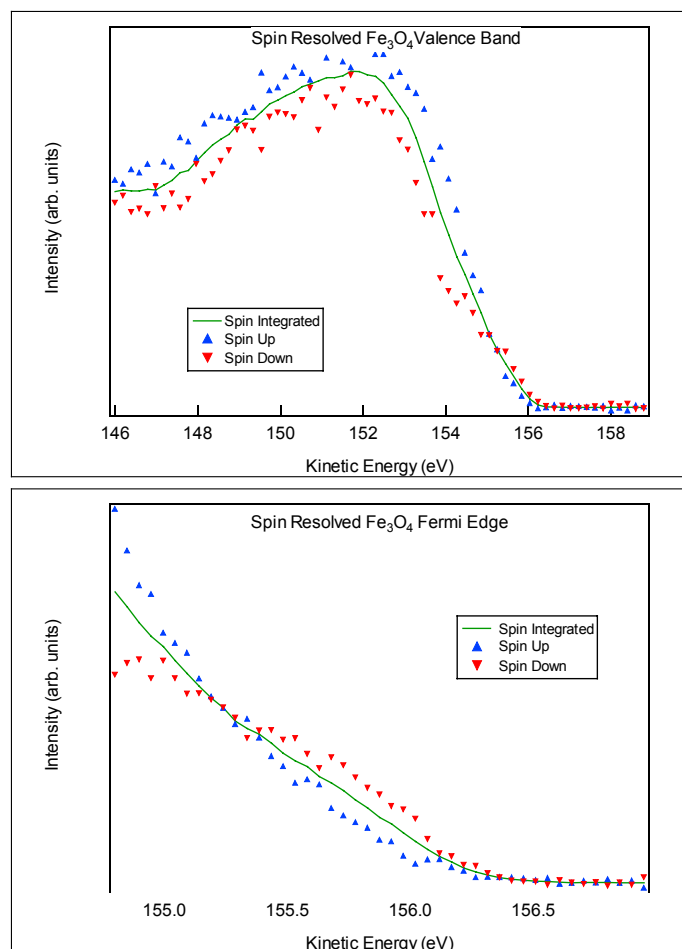


Figure 4. Spin-resolved valence band and Fermi edge for magnetite on Au(111).

REFERENCES

1. G.A. Prinz, *Science* **282**, 1660 (1998).
2. S.A. Wolf, D.D. Awschalom, R.A. Buhrman, J.M. Daughton, S. von Molnar, M.L. Roukes, A.Y. Chitchekanova, D.M. Treger, *Science* **294**, 1488 (2001).
3. Z. Zhang and S. Satpathy, *Phys. Rev. B* **44**, 13319 (1991).
4. V.I. Anisimov, I.S. Elfimov, N. Hamada, and K. Terakura, *Phys. Rev. B* **54**, 4387 (1996).
5. J.J. Versluijs, M.A. Bari, and J.M.D. Coey, *Phys. Rev. Lett.* **87**, 026601 (2001).
6. M.P. Nikiforov, A. Vertegel, M.G. Shumsky, and J.A. Switzer, *Adv. Mater.* **12**, 1351 (2000).
7. J.G. Tobin, P.J. Bedrossian, T.R. Cummings, G.D. Waddill, S. Mishra, P. Larson, R. Negri, E. Peterson, P. Boyd, and R. Gunion, *MRS Symp. Proc.* **524**, 185 (1998).
8. H.J. Kim et al., *Phys. Rev. B* **61**, 15284 (2000).
9. D.J. Huang, L.H. Tjeng, J. Chen, C.F. Chang, W.P. Wu, A.D. rata, T. Hibma, S.C. Chung, S.-G. Shyu, C.-C. Wu, and C.T. Chen, *Surf. Rev. Lett.* (in press).
10. Y.S. Dedkov, U. Rudiger, and G. Guntherodt, *Phys. Rev. B* **65**, 064417 (2002).
11. S.F. Alvarado, W. Eib, F. Meier, D.T. Pierce, K. Sattler, H.C. Siegmman, J.P. Remeika, *Phys. Rev. Lett.* **34**, 319 (1975).

The National Science Foundation (CHE 9816484, DMR 0071365, and DMR 0076338) and the Foundation for Chemical Research are gratefully acknowledged for financial support of this work.

Principal investigator: Dan Waddill, Department of Physics and Graduate Center for Materials Research, University of Missouri-Rolla. Telephone: 573-341-4797. Email: waddill@umr.edu.

Photoemission Electron Microscopy and X-Ray Magnetic Circular Dichroism of $\text{Fe}_x\text{Ni}_{(1-x)}$ Thin Films on Cu(111)

Y.Sato¹, T.F.Johnson¹, S.Chiang¹, X.D.Zhu¹, D.P.Land², J.A.Giacomo¹
F.Nolting³, and A.Scholl³

¹Dept. of Physics, University of California, Davis, CA 95616

²Dept. of Chemistry, University of California, Davis, CA 95616

³Advanced Light Source, Lawrence Berkeley National Laboratory, Berkeley, CA 94720

INTRODUCTION

Our research focuses on controlling the structure, composition and the resultant magnetic properties of metal alloy thin film growth at the atomic level. Better understanding and control of surface/interface magnetism is relevant to the application of the giant magneto-resistive effect to read heads for magnetic recording. We have studied $\text{Fe}_x\text{Ni}_{(1-x)}$ alloy thin films for their technological relevance to the above mentioned technology. The dependence of the magnetism on the stoichiometry x is one of the questions of interest. In addressing this problem, the structure of the thin film must be also considered. In terms of crystal structure, a well known “Invar effect” exists in bulk FeNi alloy because of structural incompatibilities of the two elements. Pure Fe is stable in bcc phase whereas pure Ni has fcc structure. A bulk alloy containing more than 65% Fe transforms to bcc by a Martensitic transformation, and the magnetization falls to zero. In thin film alloys, the problem may become more complex because of the effect of substrate structure and interface properties. On the other hand, how this structural change affects the magnetic order in the film is not well known. A simultaneous study of film structure, magnetic structure and magnetism is needed to better understand the system.

Several studies on $\text{Fe}_x\text{Ni}_{(1-x)}$ alloy thin films have been reported^{1,2,3,4}. Information on the growth, structure, and magnetic moments as a function of thickness and concentration has been obtained using various techniques such as low energy electron diffraction (LEED), reflection high energy electron diffraction (RHEED), photoelectron diffraction, surface magneto optical Kerr effect (SMOKE), X-ray magnetic linear dichroism (XMLD), Mossbauer spectroscopy, and superconducting quantum interference device (SQUID) magnetometry. We have used the photoemission electron microscope (PEEM2) at the Advanced Light Source (beamline 7.3.1.1) to study this film system. PEEM has the unique capability of imaging the film’s magnetic structure with high spatial resolution and elemental specificity. Simultaneously, quantitative magnetic information can be obtained using magnetic circular dichroism in X-ray absorption spectroscopy. At two different thicknesses, we have made sixteen samples and studied the dependence of magnetic structure on varying Fe concentration and substrate quality ($x = 0, 0.28, 0.55, 0.6, 0.66, 0.74, 1.0$ at $10\text{\AA} \approx 5\text{ML}$, $x = 0.9, 0.25, 0.33, 0.42, 0.5, 0.55, 1.0$ at $20\text{\AA} \approx 10\text{ML}$). We have observed clear ferromagnetic domain structures of the film on a Cu(111) surface for $x \leq 0.60$ at room temperature.

RESULTS

Samples with high Fe content ($x=0.66, 0.74$ at 5ML) have been observed to be non-magnetic at room temperature. All other alloy samples ($x \leq 0.6$, 5ML and 10ML) showed clear ferromagnetic contrast. This trend of reduction in Curie temperature at higher Fe concentration is also observed by spin resolved photoemission spectroscopy measurements carried out at the Advanced Light Source (beamline 7.0.1.2). A pure Ni film at 5ML thickness was non-magnetic at room temperature. According to a SMOKE measurement, 5ML is approximately the thickness where the Curie temperature becomes less than room temperature for Ni/Cu(111)⁵.

Fig. 1 shows typical ferromagnetic images with a $12\mu\text{m}$ field of view for a 5ML thick $\text{Fe}_{0.6}\text{Ni}_{0.4}$ film on Cu(111). Each image is obtained by dividing an image acquired at the L3 Fe (or Ni) edge by one acquired at the L2 Fe (or Ni) edge. The images show alignment of the magnetic domains for

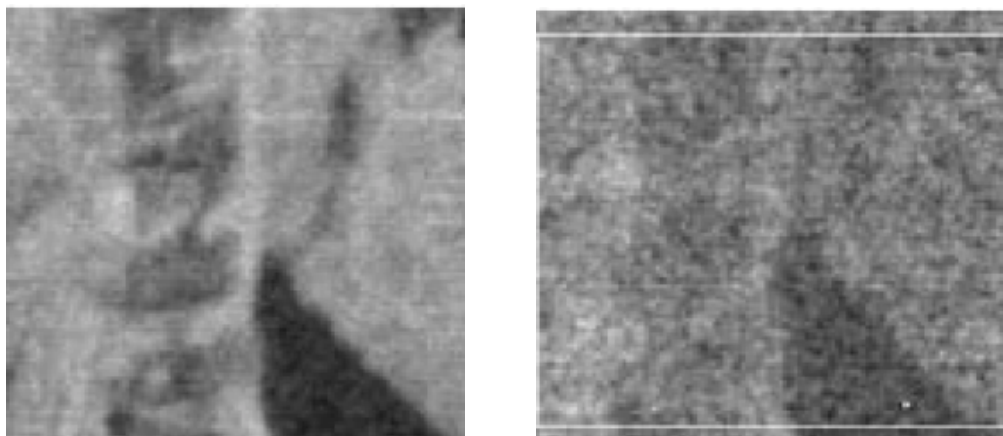


Fig. 1. XMCD ferromagnetic images with a $12\mu\text{m}$ field of view for a 5ML thick $\text{Fe}_{0.6}\text{Ni}_{0.4}/\text{Cu}(111)$. Left: Fe XMCD contrast, Right: Ni XMCD contrast.

Fe and Ni, suggesting that Fe and Ni form a good alloy on this surface. By comparing the images shown in Fig. 2 and Fig. 3, we find a clear dependence of the domain structures on film thickness and substrate quality. Fig. 2 shows magnetic contrast images of 5ML alloy films on a mechanically polished substrate. On these samples, observed magnetic structures appear to correlate to surface topographic features. No regular appearance of domain structure was seen. Comparison of the image at the pre-absorption edge, which shows only topographic contrast, with the magnetic contrast image clearly shows the correlation between surface structural features and the formation of magnetic domains. An experiment showed that magnetic contrast observed at room temperature disappears gradually upon heating. Contrast is recovered again as the sample temperature is lowered below the Curie temperature. This also confirms the relation between domain structure and surface geometric structures. These observations are consistent for each 5ML sample analyzed. In contrast, for 10ML films on an electropolished substrate as shown in Fig. 3, pinning due to surface defects is observed less frequently. Magnetic structures and textures appear to be more uniform and the sizes of the structures were smaller and on the order of $1\text{-}3\mu\text{m}$. At the alloy composition of $x=0.44$, regular, periodic appearance of larger domain structures ($5\text{-}10\mu\text{m}$ width and $70\mu\text{m}$ length), defined by 180° domain walls, are observed, as shown in Fig. 4. By observing the two images shown in Fig. 4, we conclude that alloy film at this composition and thickness show in-plane magnetization.

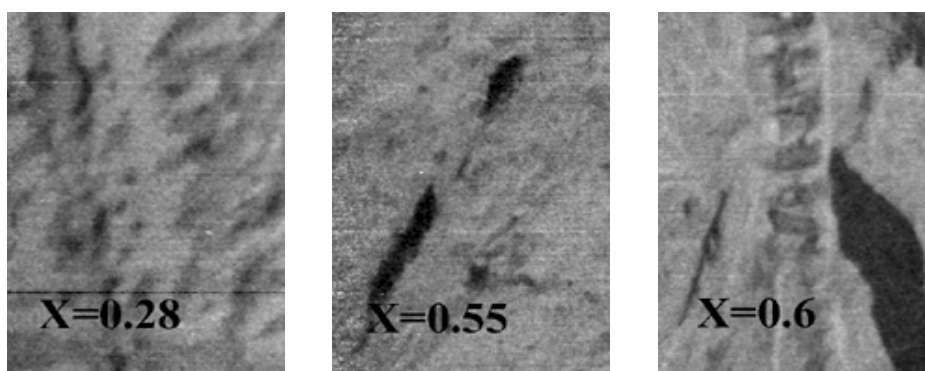


Fig. 2. XMCD ferromagnetic images with $H22\mu\text{m} \times V30\mu\text{m}$ field of view for 5ML films with varying Fe composition x .

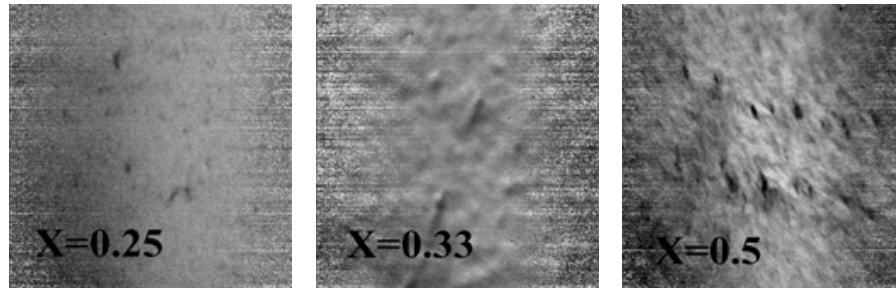


Fig. 3. XMCD ferromagnetic images with $65\mu\text{m} \times 65\mu\text{m}$ field of view for 10ML films with varying Fe composition x .

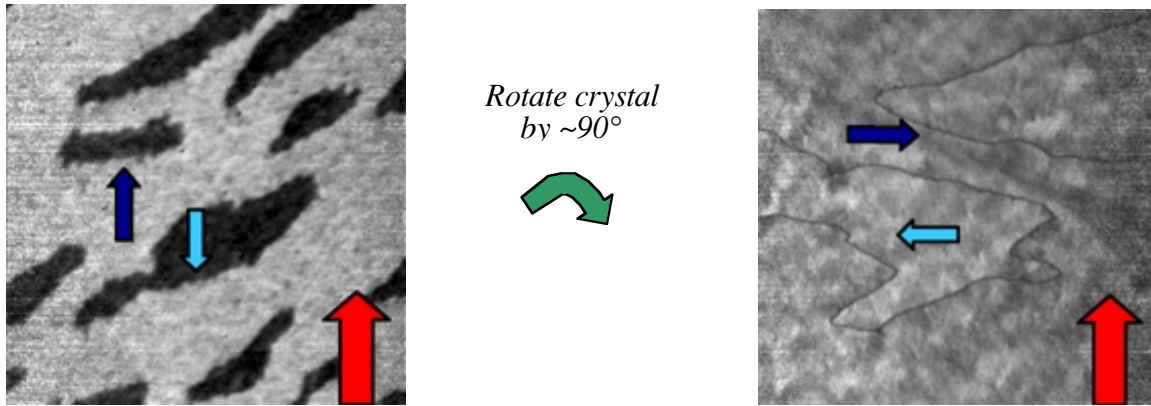


Fig. 4. XMCD ferromagnetic images with Right: $45\mu\text{m} \times 45\mu\text{m}$ and Left: $45\mu\text{m} \times 45\mu\text{m}$ field of view for 10ML thick $\text{Fe}_{0.56}\text{Ni}_{0.44}/\text{Cu}(111)$. Smaller arrows indicate the magnetization direction and larger arrows show the direction of the incident photon momentum.

REFERENCES

1. F.O.Schumann, S.Z.Wu, G.J.Mankey, and R.F.Willis *Phys. Rev. B* **56** 2668 (1997)
2. F.O.Schumann, R.F.Willis, K.G.Goodman, and J.G.Tobin *Phys. Rev. Lett.* **79** 5166 (1997)
3. J.W.Freeland, I.L.Grigorov, and J.C.Walker *Phys. Rev. B.* **57** 80 (1998)
4. R.Schellenberg, H.Meinert, N.Takahashi, F.U.Hillebrecht, and E.Kisker *J. App. Phys.* **85** 6214 (1999)
5. R.Zhang, and R.F.Willis *Phys. Rev. Lett.* **86** 2665 (2001)

This work was supported by the Campus Laboratory Collaboration Program of the University of California Office of the President and by the Director, Office of Energy Research, Office of Basic Energy Sciences, of the U.S. Department of Energy under Contract No. DE-AC03-76SF00098.

Principal investigator: Shirley Chiang, Department of Physics, University of California, Davis, CA 95616-8677.
Email: chiang@physics.ucdavis.edu. Telephone: 530-752-8538.

Spin-resolved electronic structure studies of ultrathin films of Fe on singular and vicinal GaAs

M. Spangenberg¹, E.A. Seddon¹, E.M.M. McCash², T. Shen³,
S.A. Morton⁴, D. Waddill⁵ and J. Tobin⁴

¹CLRC Daresbury Laboratory, Keckwick Lane, Daresbury, Cheshire, UK

²Department of Chemistry, University of York, Heslington, York, UK

³Joule Physics Laboratory, University of Salford, Salford, Greater Manchester, UK

⁴Lawrence Livermore National Laboratory, 7000 East Ave., Livermore, CA 94550

⁵Department of Physics, University of Missouri-Rolla, Rolla, MO 65409

Recently, there has been considerable interest in the study of spin injection at ferromagnetic semiconductor heterojunctions and ferromagnetic metal – semiconductor contacts^{1,2,3,4}. Studies of n-type semiconductors have demonstrated spin-coherent transport over large distances⁵ and the persistence of spin coherence over a sizeable time scale⁶. Clearly such investigations have been stimulated by the potential of the development of ‘spintronics’, electronic devices utilising the information of the electron spin states. To understand and improve the magnetic properties of ultrathin Fe films on GaAs has been the aim of many research groups over recent years. The interest in this system has both technological and fundamental scientific motivations. Technologically, Fe on GaAs may serve to realize spin electronic devices. From a fundamental science point of view, Fe on GaAs serves as a prototype for studies of the interplay between the crystalline structure and morphology of an ultrathin film, its electronic structure and the long range magnetic order it exhibits.

In contrast to the attention given to Fe on variously prepared GaAs substrates, the magnetism of Fe on vicinal GaAs substrates has received scant attention. This in spite of the fact that films grown on vicinal substrates present a number of advantages and opportunities. For example, they are known to exhibit enhanced structural homogeneity, surface diffusion tends to follow well mapped patterns (the quasi-periodicity has been exploited to produce quantum wires) and there is an additional degree of control of the film growth beyond those associated with temperature and substrate surface composition⁷.

In a preliminary combined spin-polarized secondary electron spectroscopy, photoelectron spectroscopy and LEED study (carried out on the SRS, Daresbury Laboratory) of the remanent magnetic properties of Fe on singular and vicinal (3° offset) GaAs we have shown both that the various magnetic phases formed are dependant upon the Ga to As surface composition of the substrate and that they evolve in characteristic (but not well understood) ways with Fe overlayer thickness⁸. A remarkable feature in this system, which illustrates the importance of the Fe overlayer/substrate interaction, is the magnetic anisotropy; the easy axis of the Fe films on Ga-terminated substrates is perpendicular to that for As-terminated substrates^{9,10}.

These measurements were followed up with combined spin-resolved photoemission and magnetic linear dichroism experiments on Fe deposited on vicinal (offset by 3° and 6°) or singular GaAs substrates on Beamline 7 at the ALS in collaboration with Elaine Seddon of CCLRC Daresbury Laboratory, Dan Waddill of The University of Missouri-Rolla and James Tobin Of Lawrence Livermore National Laboratory. The GaAs(100) substrates were available for film deposition at room temperature after substrate decapping *in-situ* (by thermal annealing),

at the ALS. By mounting both singular and vicinal GaAs substrates on the same sample tile the same growth conditions applied for both films facilitating direct comparison. The surface quality was monitored using LEED. The following data were obtained, high resolution spin-integrated valence bands, the spin-resolved valence bands and their energy dispersion, the film thickness dependence of the spin-resolved valence bands, magnetic linear dichroism data on the Fe3p and Fe2p core levels at a variety of photon energies.

The experiments, which were performed with Dr. Simon Morton and Dr. Jim Tobin in November of 2000 have produced considerable amount of interesting results. The significant differences in the spin-resolved valence bands between *ca.*20 Å thick Fe films on singular and vicinal (3°) GaAs are illustrated in Fig.1. As the terrace width is *ca.*55 Å the spectral differences are not due to step-localized features.

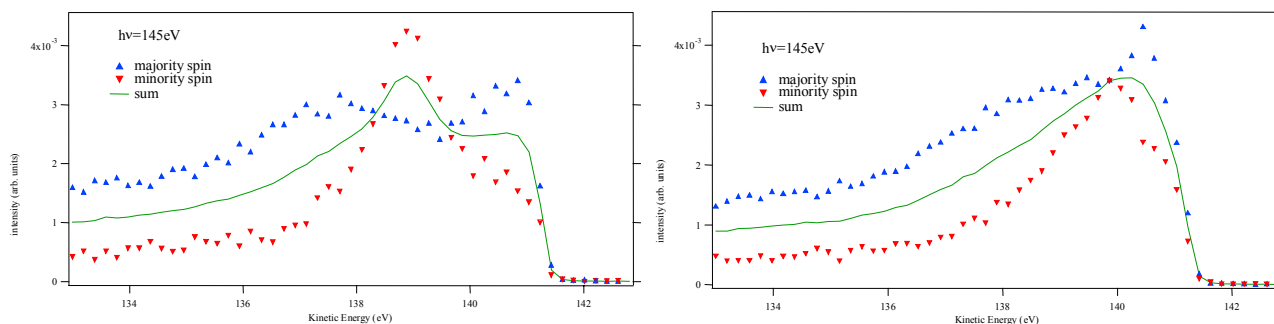


Figure 1
Spin-resolved valence band photoemission results for Fe on singular GaAs (left) and Fe on vicinal (3°) GaAs (right).

Other interesting results include the following. At low film thicknesses, Fe deposited on singular substrates was found to have a lower Curie temperature than Fe on vicinal substrates. Fe deposited on singular substrates reveals a larger energy dispersion of the spin-resolved valence bands than Fe on vicinal substrates. Only marginal differences can be seen between the spin-resolved valence bands of Fe deposited on 3° stepped GaAs substrates and Fe deposited on 6° stepped GaAs substrates. Also, in contrast to the valence band studies, the linear magnetic dichroism results obtained for these samples are very similar.

Further experiments at ALS during oct 2001 enabled us to obtain considerably more interesting results. Whilst the detailed analysis of the results is still underway, Fig.2 shows a large contrast of the valence band spectra of Fe versus incident photon energy between that on a singular and a vicinal substrate. The strong feature on the left in Fig.2 was found to be sensitive to the thickness of the Fe layer and the origin of which is still not yet clear at the present stage.

In summary, the experiments at the ALS have been extremely rewarding. They have answered some questions, clarified our thinking on others and raised yet other questions for which we have no answers at the moment. The run has, however, shown that further access to the ALS is needed to fully understand this fundamental and technologically important system.

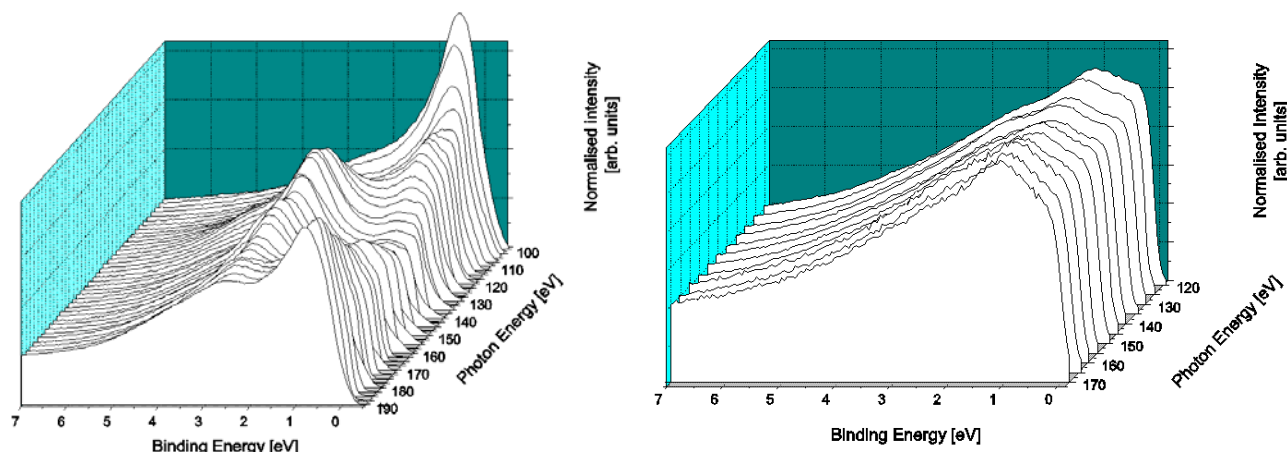


Figure 2.

Valence band spectra of Fe, normalised to the secondary electron tails, versus photon energy for films on singular substrate (left) and on 6 degree vicinal substrate (right).

References:

- ¹ Malajovich I., Berry J.J., Samarth N. and Awschalom D.D., *Nature* 411, 770 (2001)
- ² Ohno Y., Young D.K., Beschoten B., Matsukura F., Ohno H. and Awschalom D.D., *Nature* 402, 790 (1999)
- ³ Filip A.T., Hoving B.H., Jedema F.J., van Wees B.J., Dutta B. and Borghs S., *Phys. Rev. B* 62, 9996 (2000)
- ⁴ Hammar P.R., Bennett B.R., Yang M.Y. and Johnson M., *Phys. Rev. Lett.* 83, 203 (1999)
- ⁵ Kikkawa J.M. and Awschalom D.D., *Nature* 397, 139 (1999)
- ⁶ Kikkawa J.M. and Awschalom D.D., *Phys. Rev. Lett.* 80, 4313 (1998)
- ⁷ Joyce B. A., Neave J. H., Zhang J., Vvedensky D. D., Clarke S., Hugill K.J., Shithara T. and Myers-Beaghton A.K., *Semicond. Sci. Technol.*, **5** 1147 (1990). Kawamura T., Maruta J. and Ishii A., *J. Appl. Phys.*, **39** (7B) 4376 (2000). Gaines J.M., Petroff P.M., Kroemer H., Simes R.J., Geels R.S. and English J.H., *J. Vac. Sci. Technol.*, **B6** 1373 (1998).
- ⁸ Zhang T., Spangenberg M., Greig D., Takahashi N., Shen T-H., Matthew J.A.D., Cornelius S. M., Rendall M. and Seddon, E.A., *Appl. Phys. Letters*, **78** 961 (2001)
- ⁹ Kneedler E. M., Jonker B. T., Thibado P. M., Wagner R. J., Shanabrook B. V., and Whitman L., *J. Phys. Rev. B*, **56** 8163 (1997).
- ¹⁰ Gester M., Daboo C., Hicken R. J., Gray S. J., Ercole A., and Bland J. A. C., *J. Appl. Physics* **80** 347 (1996).

This work was supported by the Director, Office of Energy Research, Office of Basic Energy Sciences, Materials Science Division, of the U.S. Department of Energy under Contract No. # R5-32633.A02. This work was performed under the auspices of the U.S Department of Energy by Lawrence Livermore National Laboratory under contract no. W-7405-Eng-48. Experiments were carried out at the Spectromicroscopy Facility (Beamline 7.0) at the Advanced Light Source, built and supported by the Office of Basic Energy Science, U.S. Department of Energy.

Principal investigator: E. A. Seddon, CCLRC Daresbury Laboratory, Daresbury, Warrington Cheshire, WA4 4AD, UK, Email: e.a.seddon@dl.ac.uk, Telephone: +44 1925 603245, fax +44 1925 693124

Variable Moments and Changing Magnetic Behavior of Thin-Film FeNi Alloys

M. Hochstrasser¹, J.G. Tobin¹, N.A.R. Gilman², R.F. Willis², S.A. Morton³, and G.D. Waddill³

¹Chemistry & Material Science Division, Lawrence Livermore National Laboratory,
Livermore, California 94550, USA

²Department of Physics, The Pennsylvania State University, University Park, Pennsylvania 16802, USA

³Department of Physics, University of Missouri-Rolla, Rolla, Missouri 65409, USA

INTRODUCTION

The electronic properties and magnetic behavior of FeNi alloys have been of special interest since 1897 when Guillaume [1] first reported an almost zero thermal expansion over a wide temperature range in face-centered cubic (fcc) crystals with a Ni concentration of around 35 atomic percent. This behavior was subsequently observed in various ordered and random binary alloy systems, and became known as the “Invar Effect” [2]. Despite much experimental [3] and theoretical [4] work, a full understanding of this important technological effect is lacking.

A general view, first advanced by Weiss [3], is that the Fe atoms first develop a large magnetic moment in the Ni-rich alloys, which expands their lattice as their number increases. At a critical Wigner-Seitz cell volume, the strain energy becomes too large and there is a phase transition from this “high-spin/high-volume” state into a ‘low-spin/low-volume’ state. In the bulk alloys, this instability begins around 60% Fe content, the Curie temperature falling precipitously, simultaneously with a ‘martensitic’ structural transformation to body-centered cubic (bcc) symmetry [2]. Theoretical work predicts that the fcc phase can exist in two possible states: a ferromagnetic high volume state or an antiferromagnetic low volume state (2 γ state model) [3] with a volume change between the paramagnetic and the high spin state of $\sim 7\%$ [5], and 1% change between a non-collinear equilibrium state and the high spin state [4]. Experimental work shows a lattice expansion increasing linearly up to 3% at 65% Fe content followed by a sudden relaxation of 2% with increasing Fe content [6]. This work also shows that the martensitic structural transformation can be arrested in ultrathin alloy films epitaxially grown on a Cu(100) substrate. The nanometer-scale thickness effectively ‘clamps’ the crystal structure to that of the fcc substrate. Small changes in the Wigner-Seitz cell volume produce a small tetragonal distortion, which can be monitored by diffraction methods [6]. By growing ultrathin pseudomorphic fcc films, it is possible to focus on the effect of changing alloy composition on the magnetic and electronic behavior.

Here, we report changes in the magnitudes of both elemental magnetic moments with changing composition, measured with X-ray linear/circular dichroism as well as changes in the exchange splitting measured with spin- and angle-resolved photoemission.

RESULTS AND DISCUSSION

A plot of the change in the asymmetry amplitude, for both elements in the FeNi alloy measured with XMLDAD, being a measure of the expectation value of the atomic magnetic moment $\langle \mu \rangle$, is shown plotted as a function of composition, fig. 1 (left panel). We observe that both the Ni and Fe signals track a similar profile with changing composition. In the Ni-rich alloys, both signals increase linearly up to 65% that on the Fe showing the larger increase. Above 65% Fe content, both signals show a sharp decrease. The observed asymmetry amplitudes, suggest that a high-spin moment develops on the Fe with increasing Fe content that increases overall magnetization,

which then increases the polarization of the valence states surrounding the Ni atomic cores. The Ni thus develops a component that tracks the developing magnetization. Above 65% Fe-content, the high-spin moment on the Fe appears to collapse to a "low-spin value", causing the overall magnetization density to be lowered, which is sensed by the reduced polarization of the valence states on the Ni. A plot of the variation of a 'stoichiometric average moment' $x A(\text{Fe}_x) + (1-x) A(\text{Ni}_{1-x})$ is shown in fig. 1 (right panel).. The behavior is very similar to that reported for the variation of the saturated moment normalized to the volume of similar fcc films on Cu(100) & Cu(111) and measured with SQUID magnetometry [7]. The solid line is the behavior reported for FeNi alloys from neutron scattering measurements [2]. We note that the Ni-rich phase extrapolates to a value around $\mu = 2.5\text{-}3.0\mu\text{B}$, a value predicted theoretically for the "high-moment" metastable fcc phase [5]. The above 'mean magnetic moment' variation, normalizing the Ni asymmetry amplitude to be equivalent to the magnetic moment of metallic Ni is tracking closely the Slater-Pauling curve, the moment increasing linearly with increasing number of holes per atom in the valence electronic states. Above 65% Fe content, the average moment shows a sharp decline into a "low-spin" magnitude state, which could be the result of a collapse of the spin moment on the Fe atoms and/or a sudden decrease in magnetization due to a non collinear rearrangement of spins.

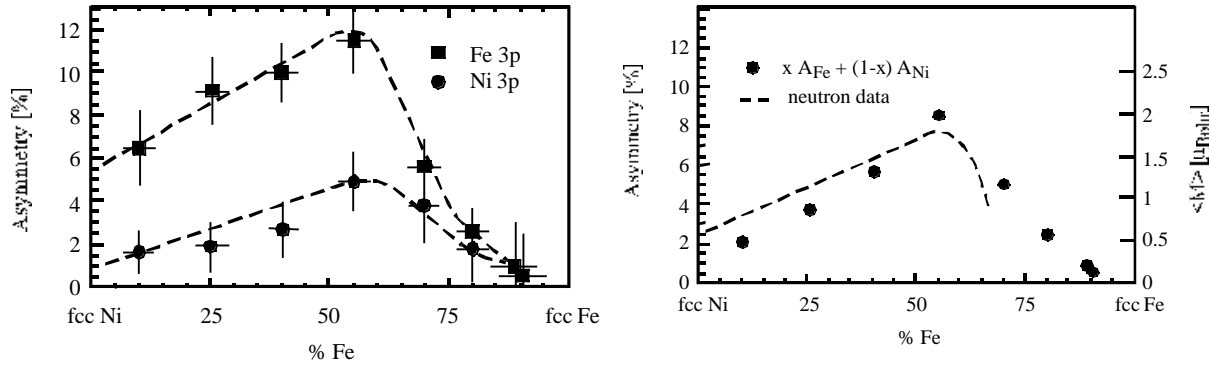


Figure 1. Left panel: Change in dichroism amplitude, A , as a function of FeNi alloy composition. Right panel: The variation of the 'stoichiometrically-weighted' dichroism signal amplitude (see text) with changing FeNi alloy composition. The dashed curve is the behavior observed in bulk FeNi alloys by neutron scattering. The right hand scale is determined from neutron and SQUID magnetometry data [2,7]

Spin polarized photoemission studies record a sudden decrease in the "mean-field" exchange splitting of the d-states with increasing Fe content through the critical "Invar transition". Angle-resolved photoemission imaging of states at the Fermi level [8] reveal a much smaller splitting of the sp-states, which also tracks the changing magnetization with changing composition. Spectral lineshapes reveal a decreased lifetime (i.e. decreased mean-free path for scattering) of the minority spin-polarized sp-states, in agreement with reported similar measurements on permalloy [9]. Angle-resolved photoemission measurements of the sp-states, away from the regions of emerging minority d-states, along the $\langle 110 \rangle$ (Σ) symmetry direction, resolves the sp exchange splitting in reciprocal space. We observe that the spectral width of the minority-spin band of the sp-states is broader than that of the majority-spin sp-band.

This has been reported in similar measurements on permalloy, and is indicative of a shorter lifetime due to increased scattering and a shorter mean-free-path for the minority spin electrons. We also note that the lifetime broadening of the minority-spin sp-states increases significantly in the Fe rich alloys. The measured exchange splitting of the sp-states as well as the spin-resolved measured exchange splitting of the d-states track the behavior of the x-ray core-level photoemission dichroism.

This is to be expected on the basis of the overall magnetic energy being the sum of a ‘local moment’ energy on the ‘atom(s) and a ‘mean-field’ exchange energy rising from the spin polarization of the itinerant valence states [10].

X-ray circular dichroism measurements allow to separate the orbital from the spin part of the local moments. Our measurements show the same concentration dependence of the local moments as the linear dichroism measurements.

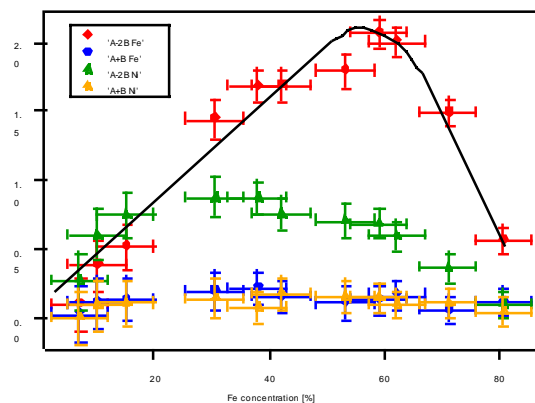


Figure 2. The variations of the spin, respectively orbital parts of the magnetic moments. $[A-2B = -C/\mu_B(\mu_s + \mu_D^{\alpha})]$; $A+B = -3C/2\mu_B(\mu_O^{\alpha})]$. A, B are the areas underneath the difference peaks of the 2p spectra taken with magnetization up and down.

REFERENCES

1. C.E. Guillaume, C.R. Acad. Sci. **125**, 235 (1897)
2. E.F. Wassermann in “Ferromagnetic Materials”, Vol. 5, K.H. Buchow & E.P. Wohlfarth (eds.), Elsevier, Amsterdam (1990)
3. R.J. Weiss, Proc. R. Soc. London, Sect. A **82**, 281 (1963)
4. M. van Schilfgaarde, I.A. Abrikosov and B. Johansson, Nature **400**, 46 (1999)
5. I.A. Abrikosov, O. Erikson, P. Sonderling, H.L. Skriver, & B. Johansson, Phys. Rev. **B51**, 1058 (1995)
6. F.O. Schumann, R.F. Willis, K.G. Goodman, & J.G. Tobin, Phys. Rev. Lett. **79**, 5166 (1997)
7. J.W. Freeland, I.L. Grigorov, & J.C. Walker, Phys. Rev. **B57**, 80 (1998)
8. M. Hochstrasser, N. Gilman, R.F. Willis, F.O. Schumann, J.G. Tobin, & E. Rotenberg, Phys. Rev. **B60**, 17030 (1999)
9. D.Y. Petrovykh, K.N. Altmann, H. Höchst, M. Laubscher, S. Maat, G.J. Mankey, & F.J. Himpsel, Appl. Phys. Lett. **73**, 3459 (1998)
10. “Ferromagnetism” by R.M. Bozorth, Van Nostrand (1951)

This work was supported by the Director, Office of Energy Research, Office of Basic Energy Sciences, Materials Science Division, of the U.S. Department of Energy under Contract No. # R5-32633.A02. This work was performed under the auspices of the U.S. Department of Energy by Lawrence Livermore National Laboratory under contract no. W-7405-Eng-48. Experiments were carried out at the Spectromicroscopy Facility (Beamline 7.0) and at Beamline 4 at the Advance Light Source, built and supported by the Office of Basic Energy Science, U.S. Department of Energy.

Principal investigator: J.G. Tobin, Chemistry & Material Science Division, Lawrence Livermore National Laboratory, Livermore, California 94550, USA, Email: tobin1@llnl.gov, Telephone: 925 422 7247

X-ray Magnetic Linear Dichroism of Fe-Ni Alloys on Cu(111)

T.F. Johnson,^{*} Y. Sato,^{*} S. Chiang,^{*} M. Hochstrasser,[#] J.G. Tobin,[#] J.A. Giacomo,^{*}
J.D. Shine,^{*} X.D. Zhu,^{*} D.P. Land,^{**} D.A. Arena,[†] S.A. Morton,^{*} G.D. Waddill^{*}

^{*}Dept. of Physics, University of California, Davis

^{**}Dept. Of Chemistry, University of California, Davis

[#]Lawrence Livermore National Laboratory, Livermore

[†]University of Missouri, Rolla

[‡]Brookhaven National Laboratory, Upton, NY

INTRODUCTION

We are studying layer-by-layer synthesis of ultra-thin metal films by controlling at the monolayer level the composition and structure of these films, including the interfacial region. We have prepared $\text{Fe}_x\text{Ni}_{1-x}$ multilayers using simultaneous evaporation of pure Fe and Ni on Cu(111) in order to better understand the Giant Magnetoresistance (GMR) effect in FeNi/Cu systems that are relevant to magnetic disk drive heads. Using Undulator Beamline 7.0 and the Spin Spectroscopy Facility (7.0.1.2) at the ALS, we have measured X-ray Magnetic Linear Dichroism (XMLD) signals for twenty three different thin Fe-Ni alloys films on Cu(111) for different thicknesses and with Fe concentration ranging from 9% to 84%. X-ray Photoelectron Spectroscopy (XPS) with 1250 eV photon energy was utilized to determine both thickness and elemental composition. The Fe3p and Ni3p lines were measured for magnetization up and down, and the difference is the XMLD signal. Our XMLD spectra clearly indicate that samples of specific thicknesses and Fe concentrations are ferromagnetic. XMLD has previously been used to characterize $\text{Fe}_x\text{Ni}_{1-x}$ alloy fcc multilayers on Cu(100)¹.

RESULTS

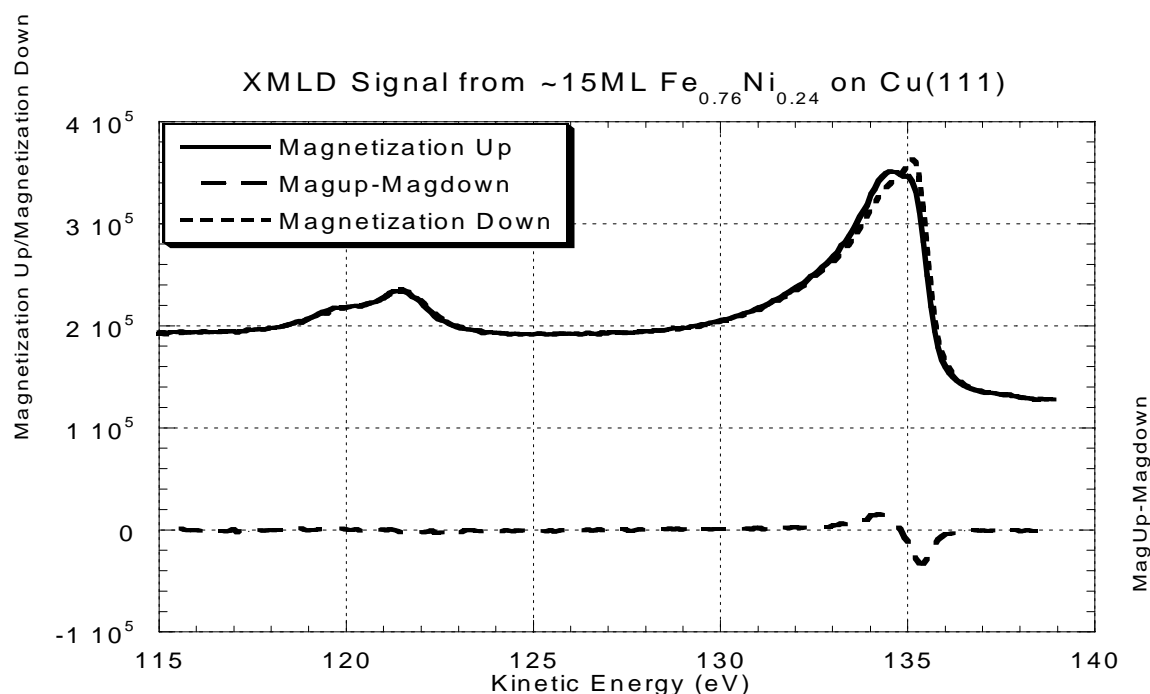


Figure 1. XMLD data from Fe-Ni thin film, 15ML thick, on Cu(111). Top of figure shows the signal for both magnetizations up and down. Bottom of figure shows difference, which is proportional to the dichroism.

Fig. 1 shows the XMLD effect for Fe concentration of 0.76 and thickness of 14ML. The upper panel clearly shows that the XPS data are different depending on the orientation of the applied field relative to the sample. The lower panel shows the difference between the two spectra in the upper panel and exhibits the dichroism effect. We have also measured the dichroism signal from both the Fe and the Ni peaks, which allows for calculation of the asymmetry.

The asymmetry is defined as, $\frac{\text{MagUp} - \text{MagDown}}{\text{MagUp} + \text{MagDown}}$, as measured from the XMLD signal.

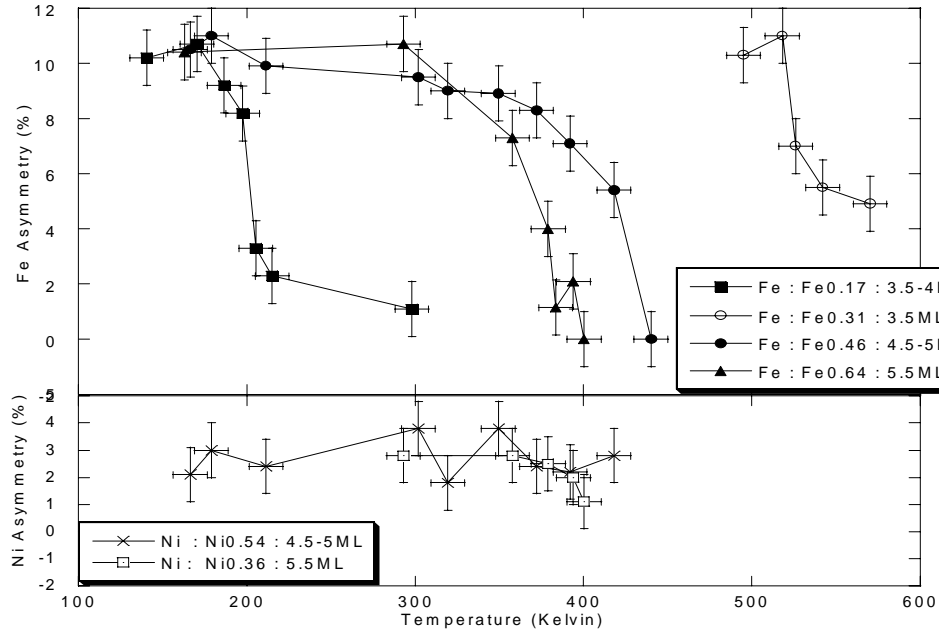


Figure 2. Fe and Ni asymmetry as a function of temperature for four Fe concentrations with film thicknesses near 5ML.

Figure 2 shows the asymmetry as a function of temperature for films with four different Fe concentrations and two different Ni concentrations, all ~5ML thick. The Fe data appear to fit the predictions from mean field theory, and preliminary attempts at mean field fits have had limited success. With increasing Fe concentration, the Curie temperature, where the asymmetry disappears, increases until $x \approx 0.6$, (near the Invar transition point) and then decreases.

Fig. 3 shows the total weighted asymmetry, A_T , which is computed by performing a weighted sum of elemental asymmetries to obtain²,

$$A_T = xA_{\text{Fe}} + (1-x)A_{\text{Ni}},$$

with A_{Fe} and A_{Ni} being the asymmetries measured from the XMLD spectra for Fe and Ni respectively. Note that A_T also shows a magnetic instability near $x=0.65$. The data also support similar results by Schumann *et al* for FeNi on Cu(001). We observe that as the Fe concentration increases, we observe A_T to have an initial value of about 2%, which then monotonically increases to a maximum of about 8.5% at the Invar transition concentration. For Fe concentrations greater than $x=0.65$, the weighted asymmetry is quenched. As the system goes through the quenching transition, it goes from a highly aligned, high spin state to an admixture

that includes a low spin state for the Fe. For Fe on CuAu(100) multilayers, Keavney *et al*³ also found high Fe asymmetry for Fe concentration less than or equal to 60%.

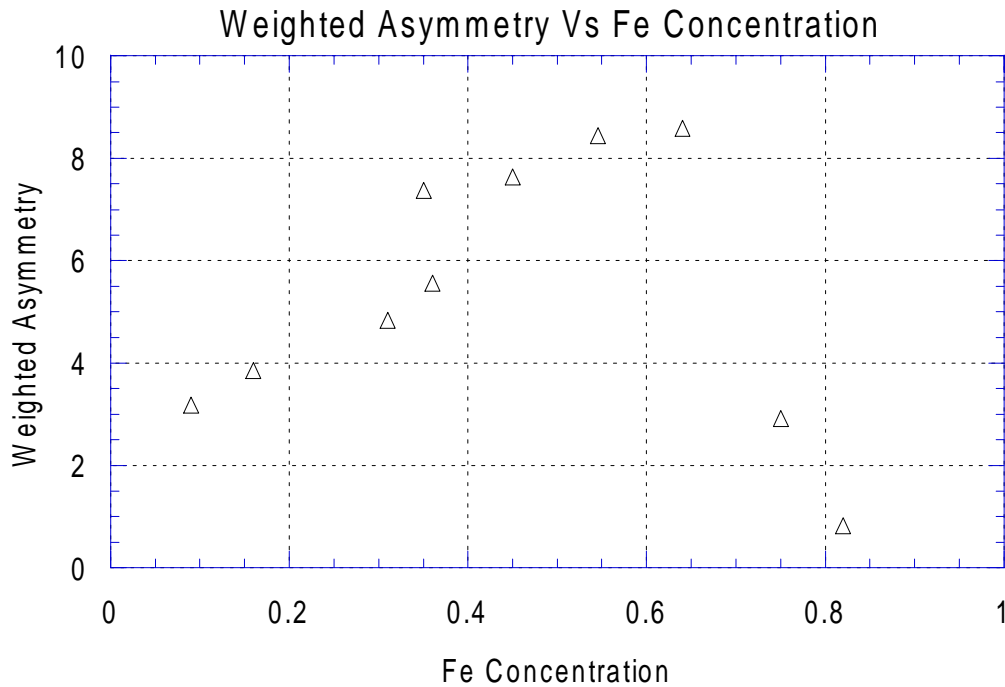


Fig. 3 Total weighted asymmetry of FeNi alloy as a function of Fe concentration for film thicknesses near 5 ML

Work is progress to compare the data in Figure 3 with previously published SQUID measurements⁴ for FeNi films on Cu(111) in order to perform an absolute calibration of the XMLD signal.

REFERENCES

1. F. O. Schumann, R. F. Willis, K. G. Goodman, J. G. Tobin, Phys. Rev. Lett., **79**, 5166 (1997).
2. F. O. Schumann, R. F. Willis, J. G. Tobin, J. Vac. Sci. Tech. A **18**, 1259 (2000).
3. D. J. Keavney, D. F. Storm, J. W. Freeland, I. L. Grigorov, J. C. Walker Phys. Rev. Lett., **74**, 4531 (1995).
4. J. W. Freeland, I. L. Grigorov, and J. C. Walker, Phys. Rev. B **57**, 80 (1998).

This work was supported by the Campus Laboratory Collaboration Program of the University of California Office of the President and was performed under the auspices of the U.S Department of Energy by Lawrence Livermore National Laboratory under contract no. W-7405-Eng-48. Experiments were carried out at the Spectromicroscopy Facility (Beamline 7.0) at the Advanced Light Source, built and supported by the Office of Basic Energy Sciences, U.S. Department of Energy.

Principal investigator: Shirley Chiang, Department of Physics, University of California, Davis, CA 95616-8677.
Email: chiang@physics.ucdavis.edu. Telephone: 530-752-8538